

# Polymerization and Decarbonylation Reactions of Aldehydes on the Pd(111) Surface

J. L. Davis and M. A. Barteau\*

Contribution from the Center for Catalytic Science and Technology, Departments of Chemistry and Chemical Engineering, University of Delaware, Newark, Delaware 19716.

Received May 26, 1988

**Abstract:** The adsorption and reaction of formaldehyde, acetaldehyde, and propanal were compared in temperature-programmed desorption (TPD) and high-resolution electron energy loss spectroscopy (HREELS) studies on a clean Pd(111) surface. Formaldehyde reacted upon adsorption at 170 K via decomposition to CO(a) and H(a) and polymerization to paraformaldehyde. In contrast, decomposition of the higher aldehydes required significantly higher temperatures. Acetaldehyde adsorbed on the clean surface in an  $\eta^2$  configuration and reacted to form stable acetyl species ( $\text{CH}_3\text{C}=\text{O}$ ), which decomposed above 300 K to produce CO(a), H(a), and  $\text{C}_1$  hydrocarbon fragments. Adsorbed acetyl groups were readily identified by the characteristic frequency of their CO stretch at  $1565\text{ cm}^{-1}$ . In competition with decarbonylation, desorption of acetaldehyde occurred at 220 and 325 K. The CO stretch of  $\eta^2$ -acetaldehyde was observed at  $1390\text{ cm}^{-1}$ . Similarly, the adlayer produced by the adsorption of propanal on Pd(111) was a mixture of  $\eta^2$ -propanal and propanoyl species ( $\text{CH}_3\text{CH}_2\text{C}=\text{O}$ ) produced by removal of the aldehyde hydrogen atom. No evidence was found for polymerization of either acetaldehyde or propanal on the clean Pd(111) surface. A kinetic isotope effect was observed in the decomposition of adsorbed acetyl intermediates, suggesting that C-H cleavage is rate determining for this reaction. These results illustrate the pathways, intermediates, and energetics of aldehyde decarbonylation reactions on group VIII metal surfaces and may provide insights into the mechanism of oxygenate synthesis from CO and  $\text{H}_2$ .

## 1. Introduction

The coordination geometry of aldehydes on surfaces of group VIII metals dramatically influences the fate of these adsorbates. Studies of aldehyde adsorption on Pt(S) [6(111)  $\times$  (100)]<sup>1</sup> and Ru(001)<sup>2</sup> have reported two coordination geometries. Aldehydes can coordinate to metal surfaces through the oxygen lone pair orbital in a monohapto,  $\eta^1(\text{O})$ , configuration (hereafter referred to simply as  $\eta^1$ ). In general, electron donation from oxygen lone pair orbital produces a relatively weak surface-adsorbate bond and, as a result,  $\eta^1$ -aldehydes typically desorb near 200 K. Other lone-pair donors such as molecularly adsorbed alcohols and ethers also interact weakly with Pd(111)<sup>3</sup> and Pt(111)<sup>4,5</sup> surfaces and desorb near 200 K. The second coordination geometry observed for aldehydes on group VIII metals is the dihapto or  $\eta^2(\text{O,C})$  configuration (hereafter referred to as  $\eta^2$ ), in which both the carbonyl carbon and oxygen atoms interact with the surface. In the  $\eta^2$  state, the aldehyde binds to the surface through the carbonyl  $\pi$  orbital, and overlap between the metal d orbitals and the carbonyl  $\pi^*$  orbital is sufficient to allow substantial electron donation from the metal to the carbonyl  $\pi^*$  orbital. The net result of this so-called "back-bonding" interaction is a strengthening of the surface-adsorbate bond and a reduction of the CO bond order of the adsorbed aldehyde. We have previously shown that the activation energy for desorption of acetone from Pd(111) was nearly 5 kcal/mol higher for  $\eta^2$ -acetone than for  $\eta^1$ -acetone.<sup>6</sup> The higher desorption temperature of  $\eta^2$  species may allow decomposition reactions to compete with desorption in TPD experiments, as observed for acetone on Pd(111). Similar observations have been reported for aldehydes adsorbed on Pt(S)[6(111)  $\times$  (100)],<sup>1</sup> Ru(001),<sup>2</sup> and Ni(100).<sup>7</sup> These two bonding configurations are not unique to aldehydes, but have been observed for other organic molecules with unsaturated heteroatom functionalities such as ketones,<sup>6,8,9</sup> fluoro ketones,<sup>10,11</sup> dimethyl sulfoxide,<sup>12</sup> and aceto-

nitrile<sup>13</sup> adsorbed on metal surfaces.

A thorough knowledge of the coordination of aldehydes to the surfaces of group VIII metals is essential to understanding the factors influencing the selectivity of oxygenate synthesis from CO and  $\text{H}_2$ . A number of mechanisms have been proposed for higher alcohol synthesis that involve aldehyde intermediates.<sup>14-16</sup> The production of higher oxygenates appears to require formation of acyl species via CO insertion into the bond between the adsorbed hydrocarbon ligands and the metal surface.<sup>14</sup> Higher oxygenate synthesis then proceeds by hydrogenation of adsorbed acyl species to produce aldehydes which either desorb as products or undergo further hydrogenation to produce alcohols. Consistent with this mechanism, TPD experiments have suggested that alcohol decomposition on Pd(111) proceeds through  $\eta^2$ -aldehyde species<sup>3</sup> in a reaction that is essentially the reverse of the mechanisms proposed for higher alcohol synthesis.<sup>14</sup> Electronegative surface modifiers have been shown to promote the binding of carbonyl compounds in an  $\eta^1$  configuration in single-crystal studies.<sup>2,6-9</sup> These observations are mirrored by those for catalytic studies which suggest that oxygenate selectivity may be enhanced by reduction of the electron density of the metal centers.<sup>17</sup> In effect, the selectivity toward oxygenated products can be increased by favoring adsorbates which lie further along the reaction coordinate toward the products (e.g.,  $\eta^1$ -aldehydes).

The influence of surface modifiers such as oxygen on the binding of organic adsorbates may be quite general. For example, aldehydes appear to be adsorbed preferentially in the  $\eta^2$ -configuration on clean surfaces of group VIII metals,<sup>1-3</sup> while adsorption of aldehydes in the  $\eta^1$  configuration appears to be favored on oxygen-dosed surfaces of these metals.<sup>2,18</sup> In an effort to un-

(1) McCabe, R. W.; DiMaggio, C. L.; Madix, R. J. *J. Phys. Chem.* **1985**, *89*, 854.

(2) Anton, A. B.; Parameter, J. E.; Weinberg, W. H. *J. Am. Chem. Soc.* **1986**, *108*, 1823.

(3) Davis, J. L.; Barteau, M. A. *Surf. Sci.* **1987**, *187*, 387.

(4) Sexton, B. A.; Rendulic, K. D.; Hughes, A. E. *Surf. Sci.* **1982**, *121*, 181.

(5) Rendulic, K. D.; Sexton, B. A. *J. Catal.* **1982**, *78*, 126.

(6) Davis, J. L.; Barteau, M. A. *Surf. Sci.*, in press.

(7) Madix, R. J.; Yamada, T.; Johnson, S. W. *Appl. Surf. Sci.* **1984**, *19*, 43.

(8) Avery, N. R. *Surf. Sci.* **1983**, *125*, 771.

(9) Anton, A. B.; Avery, N. R.; Toby, B. H.; Weinberg, W. H. *J. Am. Chem. Soc.* **1986**, *108*, 684.

(10) Avery, N. R. *Langmuir* **1985**, *1*, 162.

(11) Walczak, M. M.; Leavitt, P. K.; Thiel, P. A. *J. Am. Chem. Soc.* **1987**, *109*, 5621.

(12) Sexton, B. A.; Avery, N. R.; Turney, T. W. *Surf. Sci.* **1983**, *124*, 162.

(13) Sexton, B. A.; Avery, N. R. *Surf. Sci.* **1983**, *129*, 21.

(14) Bell, A. T. *Catal. Rev.-Sci. Eng.* **1981**, *23*, 203.

(15) Biloen, P.; Sachtler, W. M. H. *Adv. Catalysis* **1981**, *30*, 165.

(16) Ponec, V. In *Catalysis (London)* **1981**, *5*, 48.

(17) Driessen, J. M.; Poels, E. K.; Hindermann, J. P.; Ponec, V. *J. Catal.* **1983**, *82*, 26.

**Table I.** Product Yields for the Reaction of Formaldehyde on the Clean Pd(111) Surface<sup>a</sup>

| product (temp, K)                            | yield |
|--|-------|
| H <sub>2</sub> CO (260)                      | 0.1   |
| H <sub>2</sub> (300)                         | 2.1   |
| CO (470)                                     | 2.3   |
| total H <sub>2</sub> CO adsorbed and reacted | 2.4   |

<sup>a</sup> Product yields are given in units of  $10^{14}$  cm<sup>-2</sup>.

derstand the influences of surface modifiers, we have studied a number of oxygenates on both clean and oxygen-dosed Pd(111) surfaces. This paper examines the reactions of aldehydes on the clean Pd(111) surface; aldehyde oxidation pathways will be discussed elsewhere.<sup>19</sup> The effect of oxygen upon the coordination of carbonyl compounds has also been demonstrated for acetone on Pd(111).<sup>6</sup> These results and those for reactions of alcohols on Pd(111)<sup>3,18</sup> provide insights into the mechanism of oxygenate synthesis and the potential roles of surface modifiers in this reaction.

## 2. Experimental Section

The experiments were conducted in two stainless steel vacuum chambers, which have been described in detail previously.<sup>3,6</sup> Both chambers contained facilities for LEED, AES, and TPD. One chamber was equipped with a HREEL spectrometer (McAllister Technical Services) consisting of 127° cylindrical deflectors for the monochromator and analyzer sectors. HREEL spectra presented in this paper were recorded with a beam energy of 5 eV and a resolution of 56–64 cm<sup>-1</sup> at FWHM of the elastically scattered peak. Experiments examining the temperature variation of the vibrational spectra were conducted by heating under computer control to the specified temperature, followed by rapid cooling to 170 K before recording the spectrum. Generally, this process was sufficiently rapid to permit the recording of HREEL spectra at 10 K intervals without significant contamination of the surface by adsorption of gases from the chamber background. In addition, all HREEL spectra were recorded with the ionization gauge turned off in order to eliminate contamination from gases evolved from the hot filament of the gauge.

TPD spectra were collected with the aid of an IBM personal computer, which allowed up to 8 *m/e* ratios to be monitored simultaneously. A programmable power supply interfaced with the computer was used to heat the crystal linearly at the rate of 10 K/s. TPD spectra presented below have been corrected for mass spectrometer sensitivity by using standard formulas.<sup>20</sup> Absolute coverages were determined by comparison with the peak area for desorption of CO adsorbed in the  $\sqrt{3} \times \sqrt{3}R30^\circ$  overlayer, with an ideal coverage of one-third monolayer ( $5.1 \times 10^{14}$  molecules cm<sup>-2</sup>). The aldehyde adsorption temperature was 170 K in all TPD and HREELS experiments described below.

Procedures for preparation and characterization of the clean Pd(111) and surface have been described previously.<sup>3</sup> AES and LEED measurements indicated that the composition and structure of the surface were unaffected by the TPD experiments reported below.

Samples of paraformaldehyde, acetaldehyde, and propanal were stored in glass reservoirs on a dosing manifold described previously.<sup>3</sup> Formaldehyde and formaldehyde-*d*<sub>2</sub> were obtained by heating the reservoirs containing paraformaldehyde ((H<sub>2</sub>CO)<sub>n</sub>, Aldrich) and paraformaldehyde-*d*<sub>2</sub> ((D<sub>2</sub>CO)<sub>n</sub>, MSD Isotopes, 99.6%) to 360 K. These samples were thoroughly out-gassed prior to use, in order to remove trace amounts of impurities such as methanol and water. Acetaldehyde (Aldrich, 99%), acetaldehyde-*d*<sub>4</sub> (MSD Isotopes, 99.6%), and propanal (Alfa, 99%) were obtained as vapor from liquid samples and were purified by multiple freeze-pump-thaw cycles. Mass spectrometry demonstrated that all samples were free of impurities. These adsorbates were admitted to the chamber through a 1.6-mm stainless steel needle that served as a molecular-beam doser. On the basis of comparison of oxygen uptakes obtained with the Pd surface faced toward and away from the molecular-beam doser, it was determined that the doser produced a flux to the surface approximately 20 times that calculated from the background pressure in the chamber. The exposure of each of the aldehydes required for saturation of the surface was determined from exposure variation experiments; the required exposure in each case was estimated to be 10–20 langmuirs by use of the above enhancement factor for the molecular-beam doser. All data reported below were obtained following

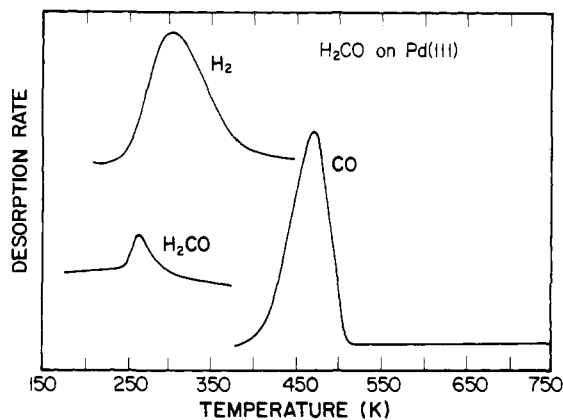


**Figure 1.** TPD spectrum observed following a saturation exposure of H<sub>2</sub>CO on the clean Pd(111) surface at 170 K.

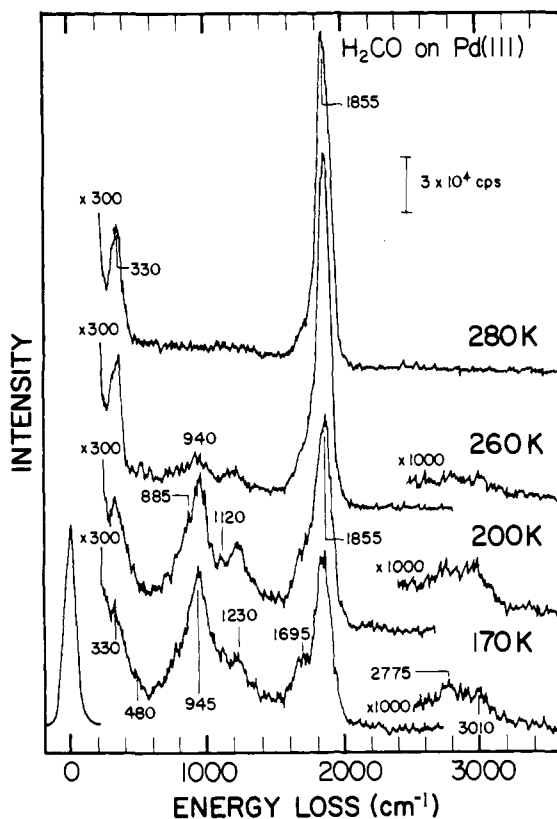


**Figure 2.** HREEL spectra of H<sub>2</sub>CO adsorbed on the clean Pd(111) surface at 170 K and upon subsequent annealing to the temperatures indicated.

saturation of the surface with the chosen reagent.

## 3. Results

**3.1. Reaction of Formaldehyde on Pd(111).** Formaldehyde decomposed to CO and H<sub>2</sub> with a high degree of conversion on the clean Pd(111) surface. As shown in the TPD spectrum in Figure 1, only a small amount of H<sub>2</sub>CO desorbed at 260 K following a saturation exposure of formaldehyde. Product yields from formaldehyde decomposition on Pd(111) are listed in Table I. The saturation coverage of formaldehyde adsorbed and reacted at 170 K was  $2.4 \times 10^{14}$  cm<sup>-2</sup> based on the carbon content of the products in TPD experiments. The principal reaction pathway observed in the TPD experiments were decomposition to adsorbed hydrogen atoms and CO. Hydrogen atoms released to the surface by H<sub>2</sub>CO decomposition recombined and desorbed at 300 K with a peak shape and desorption temperature indicative of desorption-limited kinetics. The onset of H<sub>2</sub> desorption was observed to be 230 K, consistent with that for desorption-limited H<sub>2</sub>.<sup>3</sup> The desorption of CO occurred at 470 K with a first order peak shape, consistent

(18) Davis, J. L.; Barteau, M. A. *Surf. Sci.* **1988**, *197*, 123.

(19) Davis, J. L.; Barteau, M. A., manuscript in preparation.

(20) Ko, E. I.; Benziger, J. B.; Madix, R. J. *J. Catal.* **1980**, *62*, 264.

**Table II.** Vibrational Assignments for Formaldehyde Adsorbed on Pd(111)

| mode                  | surf. species                                       | frequency, cm <sup>-1</sup> |                   |                      |                    |   |                      |                    |   |
|-----------------------|---|-----------------------------|-------------------|----------------------|--------------------|---|----------------------|--------------------|---|
|                       |   | Pd(111)                     |                   | H <sub>2</sub> CO    |                    |   | D <sub>2</sub> CO    |                    |   |
|                       |   | H <sub>2</sub> CO           | D <sub>2</sub> CO | monomer <sup>a</sup> | solid <sup>a</sup> | (H <sub>2</sub> CO) <sub>n</sub> <sup>b</sup> | monomer <sup>a</sup> | solid <sup>a</sup> | (D <sub>2</sub> CO) <sub>n</sub> <sup>b</sup> |
| $\nu(\text{CH}_2)$    | (H <sub>2</sub> CO) <sub>n</sub>                    | 3010                        | 2235              |                      |                    | 2978  |                      |                    | 2235  |
| $\nu(\text{CH}_2)$    | H <sub>2</sub> CO                                   | 2775                        | 2125              | 2782                 | 2831               |   | 2057                 | 2095               |   |
| $\nu(\text{CO})$      | CO  | 1855                        | 1825              |                      |                    |   |                      |                    |   |
| $\nu(\text{CO})$      | H <sub>2</sub> CO                                   | 1695                        | 1675              | 1746                 | 1714               |   | 1701                 | 1663               |   |
| $\delta(\text{CH}_2)$ | H <sub>2</sub> CO, (H <sub>2</sub> CO) <sub>n</sub> | nr <sup>e</sup>             | 1155              | 1500                 | 1490               | 1508 <sup>c</sup>                             | 1101                 | 1096               | 1126 <sup>c</sup>                             |
| $\rho(\text{CH}_2)$   | H <sub>2</sub> CO                                   | 1230                        | 1010              | 1249                 | 1250               |   | 998                  | 990                |   |
| $\omega(\text{CH}_2)$ | H <sub>2</sub> CO                                   |                             |                   | 1167                 |                    |   |                      |                    |   |
| $\nu_a(\text{OCO})$   | (H <sub>2</sub> CO) <sub>n</sub>                    | 1120                        | 1080              |                      |                    | 1097  |                      |                    | 1050 <sup>d</sup>                             |
| $\nu_s(\text{OCO})$   | (H <sub>2</sub> CO) <sub>n</sub>                    | 945                         | 835               |                      |                    | 932   |                      |                    | 838 <sup>d</sup>                              |
| $\rho(\text{CH}_2)$   | (H <sub>2</sub> CO) <sub>n</sub>                    | 885                         | nr                |                      |                    | 903   |                      |                    | 835   |
| $\delta(\text{OCO})$  | (H <sub>2</sub> CO) <sub>n</sub>                    | nr                          | 610               |                      |                    | 630   |                      |                    | 618   |
| $\delta(\text{COC})$  | (H <sub>2</sub> CO) <sub>n</sub>                    | 480                         | nr                |                      |                    | 455   |                      |                    | 363   |
| $\nu(\text{Pd-CO})$   | CO  | 330                         | 345               |                      |                    |   |                      |                    |   |

<sup>a</sup>IR frequencies were taken from ref 23. <sup>b</sup>IR frequencies were taken from ref 25. <sup>c</sup>Calculated vibrational frequencies from ref 25. <sup>d</sup>Strongly coupled with the  $\rho(\text{CD}_2)$  modes. <sup>e</sup>nr = not resolved.

with desorption-limited evolution of this product.

HREEL spectra collected following formaldehyde adsorption on the clean surface at 170 K indicated that the adlayer was a complex mixture, which we assign to adsorbed formaldehyde, paraformaldehyde, and CO. The HREEL spectra observed following H<sub>2</sub>CO adsorption on Pd(111) are shown in Figure 2 as a function of the temperature to which the surface was annealed. The corresponding spectra for the adlayer produced by D<sub>2</sub>CO adsorption are given in Figure 3. The presence of molecularly adsorbed CO was indicated by losses at 1855 cm<sup>-1</sup> ( $\nu(\text{CO})$ ) and 330 cm<sup>-1</sup> ( $\nu(\text{Pd-CO})$ ) in the H<sub>2</sub>CO spectrum at 170 K. In contrast, in HREELS experiments involving formaldehyde adsorption on the oxygen-dosed Pd(111) surface, no evidence was found to suggest the presence of CO(a) at temperatures below 260 K.<sup>19</sup> This observation demonstrates that the CO(a) present at 170 K following formaldehyde adsorption on the clean Pd(111) surface was produced by the reaction of formaldehyde on the surface and did not result from the adsorption of CO from the chamber background. Thus, cleavage of the carbon-hydrogen bonds of adsorbed formaldehyde to form CO(a) and H(a) occurred on Pd(111) at 170 K. Similarly, HREELS studies have demonstrated that formaldehyde adsorbs dissociatively on clean surfaces of Pt(111),<sup>21</sup> Ni(110),<sup>22</sup> and Ru(001)<sup>2</sup> at 100 K. Following formaldehyde adsorption on Pd(111), the relative intensity of the CO vibrations increased as the temperature to which the surface was annealed increased, indicating that decomposition of additional formaldehyde species occurred upon annealing the adlayer.

The presence of molecularly adsorbed formaldehyde was indicated by the CO stretching mode at 1695 cm<sup>-1</sup> in the spectrum for H<sub>2</sub>CO at 170 K. The frequency of this mode shifted slightly to 1675 cm<sup>-1</sup> in the spectrum for D<sub>2</sub>CO. These frequencies are only 40–50 cm<sup>-1</sup> below those for formaldehyde monomers in the gas phase<sup>23</sup> and are characteristic of aldehydes weakly bonded to the surface in an  $\eta^1(\text{O})$  configuration. The symmetric CH<sub>2</sub> stretching mode of molecularly adsorbed H<sub>2</sub>CO was observed at 2775 cm<sup>-1</sup>, and the CH<sub>2</sub> rocking and wagging modes appeared at 1230 cm<sup>-1</sup>. Anton et al.<sup>2</sup> have previously shown that these two modes cannot be separated for  $\eta^1$ -H<sub>2</sub>CO on the Ru(001) surface. Following adsorption of D<sub>2</sub>CO, the  $\nu_s(\text{CD}_2)$  mode was observed at 2125 cm<sup>-1</sup> and the  $\rho(\text{CD}_2)$  and  $\omega(\text{CD}_2)$  modes at 1010 cm<sup>-1</sup>. The  $\delta(\text{CH}_2)$  modes were not resolved following H<sub>2</sub>CO adsorption; however, the  $\delta(\text{CD}_2)$  mode appeared at 1155 cm<sup>-1</sup> following the adsorption of D<sub>2</sub>CO. With the exception of the asymmetric CH<sub>2</sub> stretching mode at 2843 cm<sup>-1</sup>,<sup>23</sup> all normal modes of molecular

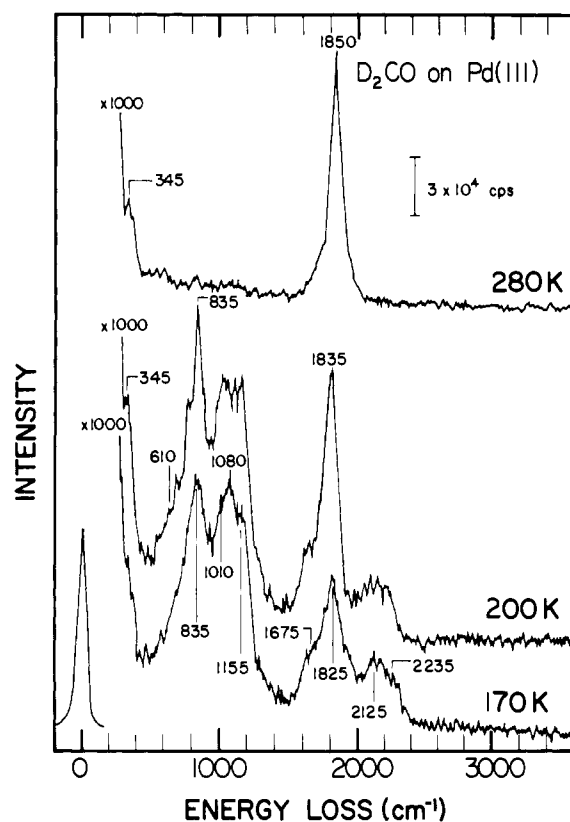


**Figure 3.** HREEL spectra for D<sub>2</sub>CO adsorbed on Pd(111) as a function of the temperature to which the adlayer was annealed.

formaldehyde were accounted for in the HREEL spectrum.

Formaldehyde adsorption on Pd(111) also produced a number of vibrations which cannot be accounted for solely by molecular formaldehyde and CO. In particular, the relatively strong loss observed at 945 cm<sup>-1</sup> following H<sub>2</sub>CO adsorption at 170 K has no analogue in the vibrational spectrum of gas-phase formaldehyde or that of molecular formaldehyde adsorbed on metal surfaces. However, these vibrations can be readily assigned to normal modes of adsorbed paraformaldehyde ((H<sub>2</sub>CO)<sub>n</sub>) produced by the polymerization of formaldehyde on the Pd(111) surface. Vibrations observed at 1120 and 945 cm<sup>-1</sup> following H<sub>2</sub>CO adsorption were assigned to the asymmetric and symmetric OCO stretches of (H<sub>2</sub>CO)<sub>n</sub>, respectively. IR studies of (D<sub>2</sub>CO)<sub>n</sub> have established that both the  $\nu_a(\text{OCO})$  and  $\nu_s(\text{OCO})$  vibrations are strongly coupled with the CD<sub>2</sub> rocking modes.<sup>25</sup> As a result, the  $\nu_a(\text{OCO})$

(21) Henderson, M. A.; Mitchell, G. E.; White, J. M. *Surf. Sci.* **1987**, *188*, 206.

(22) Richter, L. J.; Ho, W. *J. Chem. Phys.* **1985**, *83*, 2165.

(23) Khoshkoo, H.; Hemple, S. J.; Nixon, E. R. *Spectrochim. Acta* **1974**, *30A*, 863.

(24) Ibach, H.; Mills, D. L. *Electron Energy Loss Spectroscopy and Surface Vibrations*; Academic: New York, 1982.

(25) Tadokoro, H.; Kobayashi, M.; Kawaguchi, Y.; Kobayashi, A.; Murahashi, S. *J. Chem. Phys.* **1963**, *38*, 703.

mode of  $(D_2CO)_n$  adsorbed on Pd(111) was observed at  $1080\text{ cm}^{-1}$  and the  $\nu_s(\text{OCO})$  mode was observed at  $835\text{ cm}^{-1}$ . The frequency shifts observed for these vibrations are in excellent agreement with findings from IR studies of paraformaldehyde.<sup>25</sup> The  $\delta(\text{OCO})$  mode for the  $(D_2CO)_n$  adlayer was observed at  $610\text{ cm}^{-1}$  but was not resolved for  $(H_2CO)_n$ . Conversely, the  $\delta(\text{COC})$  mode of adsorbed  $(H_2CO)_n$  was observed at  $480\text{ cm}^{-1}$  but was not resolved for  $(D_2CO)_n$ . The complete assignment of the vibrations of the adlayer produced by formaldehyde adsorption on Pd(111) at 170 K is summarized in Table II along with the vibrational frequencies from previous IR studies of formaldehyde and paraformaldehyde. Paraformaldehyde was produced by the reaction of formaldehyde on the Pd(111) surface and was not the result of adsorption of paraformaldehyde from the gas phase, since mass spectrometry did not detect the presence of paraformaldehyde in the formaldehyde admitted to the vacuum chamber.

The coverage dependence of formaldehyde polymerization was also examined in HREELS experiments. For the lowest formaldehyde coverage attained ( $0.9 \times 10^{14}\text{ cm}^{-2}$ ), there were no significant differences between the HREELS spectra at this coverage and those shown in Figures 2 and 3. The polymerization of adsorbed formaldehyde on the Pd(111) surface was not coverage dependent for the formaldehyde coverages used in these experiments.

Weinberg and co-workers<sup>2</sup> have previously assigned somewhat similar spectra for  $H_2CO$  on the Ru(0001) surface to  $\eta^2\text{-H}_2\text{CO}$  rather than paraformaldehyde. They assign losses at 1160, 980, and  $840\text{ cm}^{-1}$  to the  $\omega(\text{CH}_2)$ ,  $\nu(\text{CO})$ ,  $\rho(\text{CH}_2)$  modes of  $\eta^2\text{-formaldehyde}$ , respectively. These assignments are not appropriate for the surface species derived from formaldehyde on Pd(111). First, on Ru(0001) the most intense dipole loss (assigned to the  $\nu(\text{CO})$  mode) shifts upward in frequency, from 980 to  $1020\text{ cm}^{-1}$ , upon substitution of  $D_2CO$  for  $H_2CO$ . On Pd(111) the peak with corresponding frequency and intensity shifts downward from 945 to  $835\text{ cm}^{-1}$  for the deuteriated species. We have assigned this loss above to the  $\nu_s(\text{OCO})$  mode of paraformaldehyde, which is also expected to exhibit strong dipole activity by analogy with spectra obtained for adsorbed carboxylate species.<sup>19</sup> Further, we have been able to produce  $\eta^2\text{-H}_2\text{CO}$  by decomposition of methanol on the Pd(111) surface between 170 and 240 K.<sup>26</sup> The  $\nu(\text{CO})$  mode of  $\eta^2\text{-H}_2\text{CO}$  was observed at  $1420\text{ cm}^{-1}$ , in excellent agreement with the frequencies of the corresponding modes of  $\eta^2\text{ CH}_3\text{CHO}$  and  $\text{C}_2\text{H}_5\text{CHO}$ , discussed below, and in sharp contrast to the extremely low frequency ( $980\text{ cm}^{-1}$ ) ascribed to this mode on Ru(0001).<sup>2</sup> Thus we conclude that paraformaldehyde, not  $\eta^2\text{-formaldehyde}$ , is the principal form of formaldehyde for saturation exposure of the Pd(111) surface at 170 K.

Annealing the adlayer to temperatures as high as 240 K produced relatively little change in the observed HREEL spectra. Between 240 and 260 K, vibrations of the paraformaldehyde adlayer decreased in intensity, while the intensities of the vibrations of molecularly-adsorbed CO increased. Formaldehyde desorption was observed over this temperature range in TPD experiments, suggesting that the paraformaldehyde adlayer was removed from the surface by decomposition to  $H_2CO(g)$  plus adsorbed hydrogen and CO. These observations indicate that the rate of  $H_2CO$  evolution was limited by that of paraformaldehyde decomposition. The peak temperature for  $H_2CO$  evolution from paraformaldehyde in Figure 1 was ca. 15 K greater than that for  $H_2CO$  produced by oxidation of methanol,<sup>18</sup> a reaction which does not lead to paraformaldehyde formation on this surface. Indeed, as will be shown below, formaldehyde desorption occurred at higher temperatures than that of other aldehydes adsorbed in  $\eta^1$  states. After annealing the surface to temperature above 280 K, only vibrations attributable to molecularly adsorbed CO were present. No evidence was found for the production of surface  $C_1$  hydrocarbon species via the decomposition of the paraformaldehyde adlayer, in contrast to some<sup>21</sup> but not other<sup>27</sup> reports on Pt(111).

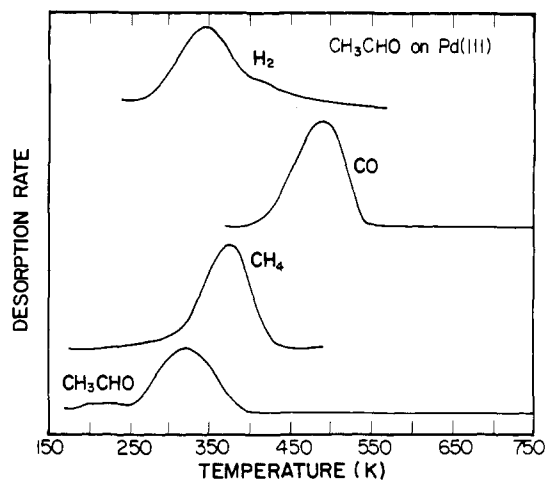


Figure 4. TPD spectrum for acetaldehyde adsorbed on the clean Pd(111) surface at 170 K.

Table III. Product Yields for the Reaction of Acetaldehyde on the Clean Pd(111) Surface<sup>a</sup>

| product (temp, K)                                  | yield |
|--|-------|
| $\text{CH}_3\text{CHO}$ (220)                      | 0.1   |
| $\text{CH}_3\text{CHO}$ (325)                      | 1.3   |
| $\text{H}_2$ (340)                                 | 2.1   |
| $\text{CH}_4$ (375)                                | 3.1   |
| $\text{H}_2$ (410)                                 | 0.1   |
| $\text{CO}$ (490)                                  | 3.8   |
| C (a)  | 0.3   |
| total $\text{CH}_3\text{CHO}$ adsorbed and reacted | 5.0   |

<sup>a</sup> Product yields are given in units of  $10^{14}\text{ cm}^{-2}$ .

**3.2. Reaction of Acetaldehyde on the Pd(111) Surface.** Acetaldehyde underwent decarbonylation on the clean Pd(111) surface to produce CO,  $\text{H}_2$ , and  $\text{CH}_4$ . Unreacted acetaldehyde desorbed in two peaks, a small peak at 220 K that was due to desorption of  $\eta^1$ -coordinated acetaldehyde and a much larger peak at 325 K due to desorption of  $\eta^2$ -acetaldehyde. The TPD spectrum following a saturation exposure of acetaldehyde on the clean Pd(111) surface is shown in Figure 4, and product yields are given in Table III. Hydrogen atoms released to the surface by the decomposition of the acetaldehyde adlayer recombined and desorbed as  $\text{H}_2$  at 340 K. The onset of  $\text{H}_2$  desorption following acetaldehyde adsorption was 270 K, 40 K higher than that observed for  $\text{H}_2$  produced by the decomposition of formaldehyde on Pd(111). The delay of the onset of  $\text{H}_2$  desorption suggests that the surface concentration of hydrogen atoms was low due to incomplete acetaldehyde decomposition. Decarbonylation of adsorbed acetaldehyde also produced methane, which desorbed at 375 K. We have previously shown that  $C_1$  hydrocarbon fragments released to the surface during the course of ethanol TPD on Pd(111) can either react with adsorbed hydrogen to produce methane or undergo sequential dehydrogenation to adsorbed carbon and hydrogen atoms.<sup>3</sup> The desorption of reaction-limited  $\text{H}_2$  at 410 K indicates that part of the  $C_1$  hydrocarbon species released to the surface upon acetaldehyde decarbonylation reacted via methylene and methyne species to produce  $\text{H}_2$  and adsorbed carbon. Further, upon completion of the TPD experiment, surface carbon was detected (as CO) by oxygen adsorption followed by temperature-programmed desorption. As shown below, acetaldehyde decomposition on the Pd(111) surface proceeds through stable acetyl ( $\text{CH}_3\text{C}=\text{O}$ ) intermediates, which have been detected previously following acetaldehyde adsorption on Pt(S)[6(111)  $\times$  (100)]<sup>1</sup> and ketene adsorption on Pt(111)<sup>28,29</sup> and Ru(0001).<sup>30</sup>

(28) Radloff, P. L.; Mitchell, G. E.; Greenlief, C. M.; White, J. M. *Surf. Sci.* **1987**, *183*, 377.

(29) Mitchell, G. E.; Radloff, P. L.; Greenlief, C. M.; Henderson, M. A.; White, J. M. *Surf. Sci.* **1987**, *183*, 403.

(26) Davis, J. L. Ph.D. Dissertation, University of Delaware, 1988.

(27) Abbas, N. M.; Madix, R. J. *Appl. Surf. Sci.* **1981**, *7*, 241.

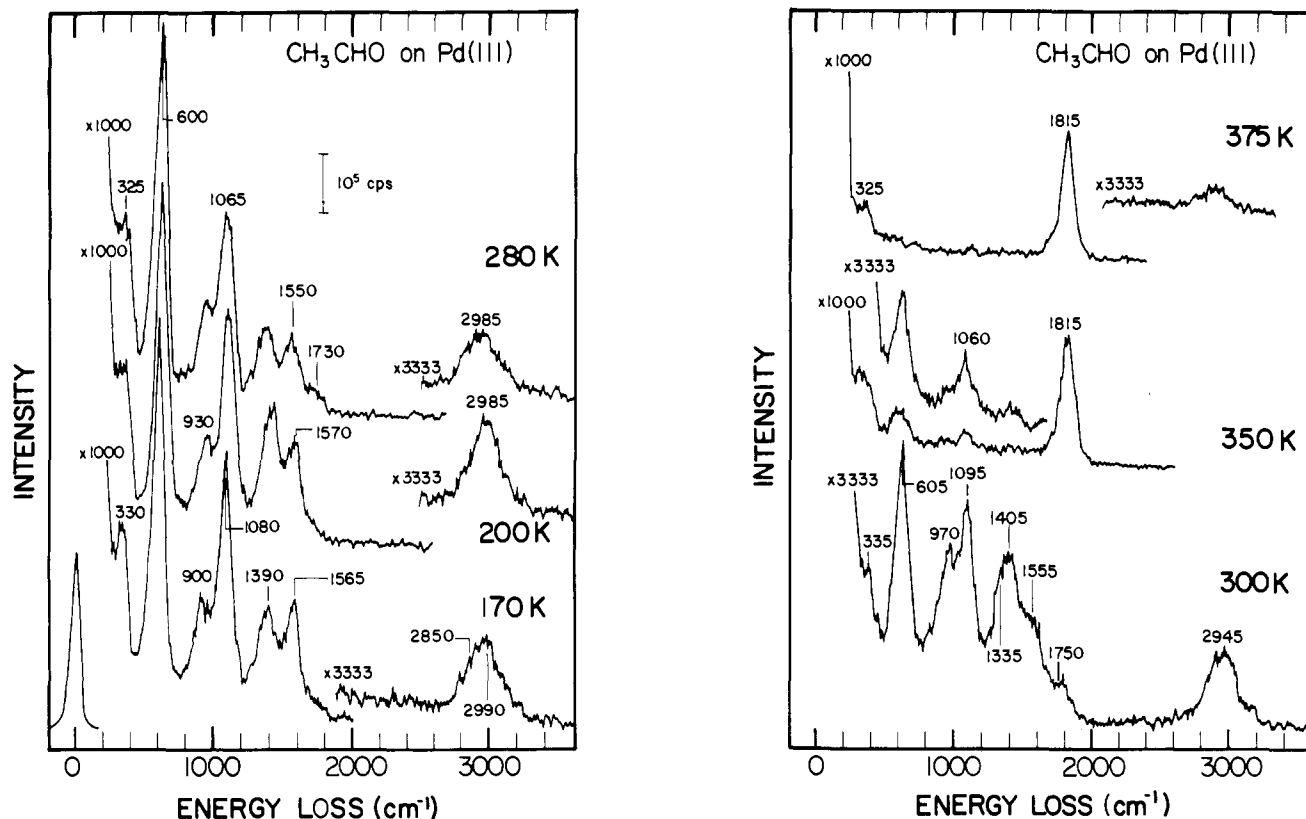


Figure 5. HREEL spectra for  $\text{CH}_3\text{CHO}$  adsorbed on the clean Pd(111) surface, followed by annealing to the temperatures indicated.

HREELS experiments provided spectroscopic evidence for the presence of both  $\eta^2$ -acetaldehyde and acetyl species following acetaldehyde adsorption at 170 K. The vibrational spectra for  $\text{CH}_3\text{CHO}$  and  $\text{CD}_3\text{CDO}$  adsorbed on the Pd(111) surface at 170 K are shown in Figures 5 and 6, respectively, along with spectra obtained as the adlayer was annealed to progressively higher temperatures. The initial coverage corresponds to the saturation value of  $5.0 \times 10^{14} \text{ cm}^{-2}$  as in Table III and Figure 4. The formation of acetyl species is demonstrated most clearly in the spectra for  $\text{CD}_3\text{CDO}$ . Following  $\text{CD}_3\text{CDO}$  adsorption on Pd(111) at 170 K, vibrations were observed at 1595 and 1400  $\text{cm}^{-1}$ . These frequencies are too high to be assigned to normal modes involving either the methyl group or the aldehyde deuteron. Instead, these losses are assigned to the  $\nu(\text{CO})$  modes of two different adsorbed species. Following adsorption of  $\text{CH}_3\text{CHO}$ , the higher frequency mode was observed at 1565  $\text{cm}^{-1}$ , but the lower frequency mode could not be unambiguously resolved from the methyl deformation modes of acetaldehyde expected between 1380 and 1430  $\text{cm}^{-1}$ . The relatively high frequencies of these modes preclude assignment to the vibrations of acetaldehyde polymers, since the CO stretching modes of paraldehyde have been reported as 1174 and 1105  $\text{cm}^{-1}$  in IR studies.<sup>31</sup> Instead, the vibration observed at 1400  $\text{cm}^{-1}$  in the spectrum of  $\text{CD}_3\text{CDO}$  at 170 K was assigned to the CO stretch of  $\eta^2$ -acetaldehyde species. This assignment is consistent with previous HREELS studies of  $\eta^2$ -acetone species adsorbed on the Pd(111) surface in which the  $\nu(\text{CO})$  mode for these species was observed at 1435  $\text{cm}^{-1}$ .<sup>6</sup>

The higher frequency mode observed at 1595  $\text{cm}^{-1}$  in the spectra following  $\text{CD}_3\text{CDO}$  adsorption was assigned to the CO stretch of adsorbed acetyl species. The frequency of the  $\nu(\text{CO})$  mode of acetyl species is expected to be higher than that of  $\eta^2$ -acetaldehyde, since removal of the aldehyde hydrogen would most likely be accompanied by an increase in the strength of the carbon-oxygen bond. Acetyl species were most likely bonded to the

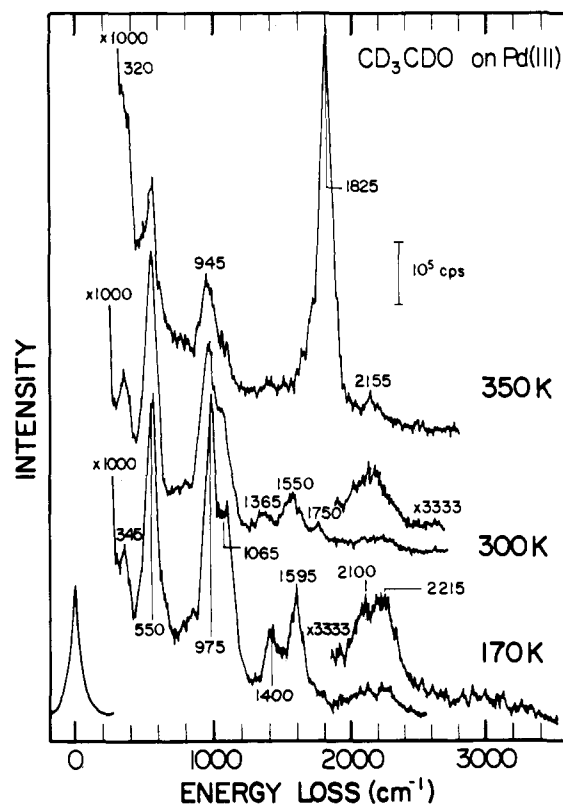


Figure 6. Variation of the HREEL spectra for  $\text{CD}_3\text{CDO}$  adsorbed on Pd(111) as the surface was annealed to higher temperatures.

Pd(111) surface through the carbonyl carbon atom, although some back-bonding must occur as evidenced by a CO stretch which is 150  $\text{cm}^{-1}$  less than the corresponding mode for gas-phase acetaldehyde. Support for the formation of stable palladium-acetyl complexes is well documented in the literature of organometallic chemistry. A number of palladium coordination compounds

(30) Henderson, M. A.; Radloff, P. L.; White, J. M.; Mims, C. A. *J. Phys. Chem.* **1988**, *92*, 4111.

(31) Fernando, J.; Boero, R.; de Mandirol, O. B. *J. Chim. Phys. Phys.-Chim. Biol.* **1976**, *73*, 163.

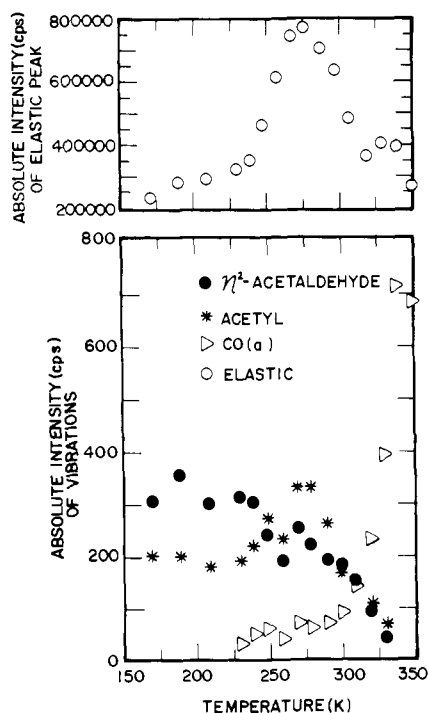


Figure 7. Temperature dependence of the vibrations of the adlayer produced by  $\text{CH}_3\text{CHO}$  adsorption on Pd(111) at 170 K. Shown in the figure are the absolute intensity of the following: (\*) the  $\nu(\text{CO})$  mode of acetyl species at  $1565\text{ cm}^{-1}$ ; (●) the  $\nu(\text{CO})$  mode of  $\eta^2$ -acetaldehyde at  $1390\text{ cm}^{-1}$ ; ( $\triangleright$ ) the  $\nu(\text{CO})$  mode of  $\text{CO}(\text{a})$  near  $1815\text{ cm}^{-1}$ ; and (○) the intensity of the elastic peak. The data were collected in a single experiment that consisted of cycles of annealing to progressively higher temperatures and quenching the reaction by cooling rapidly to 170 K.

containing acyl ligands have been synthesized.<sup>32-35</sup> The CO stretch of the acetyl ligand in these complexes ranges from  $1661$  to  $1675$ ,<sup>32,33</sup> ca.  $80\text{ cm}^{-1}$  higher than the frequency of the CO stretch observed for acetyl species adsorbed on Pd(111). Palladium-acetyl complexes are of the form *trans*-[PdX(COME)(PEt<sub>3</sub>)<sub>2</sub>], where X is a halide ligand, and the acetyl ligand is coordinated to the metal center via the coordinatively unsaturated carbonyl carbon atom (i.e.,  $\eta^1(\text{C})$  configuration). Virtually no overlap between the metal d orbitals and the carbonyl  $\pi^*$  orbital is observed for mononuclear palladium-acetyl complexes, accounting for the relatively high CO stretching frequency of these compounds. The absence of back-bonding in mononuclear Pd-acetyl compounds may be due in part to the presence of the electronegative halide ligand trans to the acetyl group. In contrast, on the Pd(111) surface, the presence of neighboring palladium atoms may permit a higher degree of back-bonding for acetyl species than is possible for mononuclear compounds.

The frequency of the CO stretch of the acetyl species produced from acetaldehyde on Pd(111) was  $80\text{ cm}^{-1}$  lower than that of  $\eta^1(\text{C})$ -acetyl ligands observed in Pd coordination compounds but higher than that of  $\eta^2$ -acetaldehyde by roughly  $180\text{ cm}^{-1}$ . Acetyl species have also been produced by the reaction of ketene ( $\text{H}_2\text{C}=\text{C}=\text{O}$ ) on the Pt(111) surface.<sup>28,29</sup> In these experiments, ketene was observed to coordinate to the surface as a di- $\sigma$ -bonded complex through the two carbon atoms. Annealing the ketene adlayer to temperatures greater than 200 K produced stable acetyl species which coordinated to the surface through the carbonyl carbon and exhibited a CO stretching frequency of  $1600\text{ cm}^{-1}$ .<sup>29</sup> The highest frequency which could be assigned to the CO stretch of acetyl species on metals which produce a higher extent of back-bonding is at correspondingly lower frequencies: at  $1480$

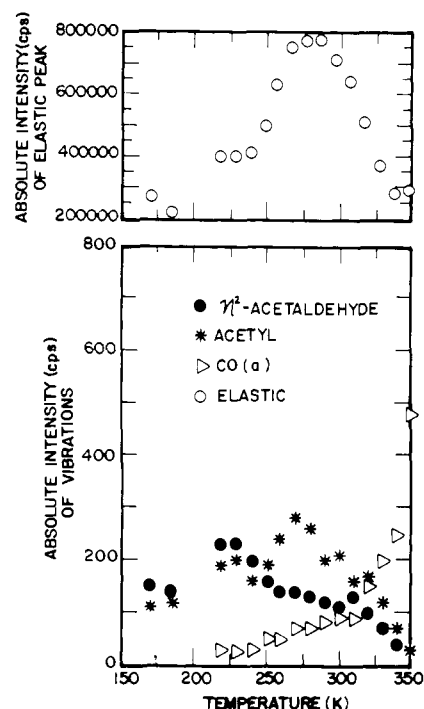


Figure 8. Temperature dependence of the vibrations of the adlayer produced by  $\text{CD}_3\text{CDO}$  adsorption on Pd(111) at 170 K. Shown in the figure are the absolute intensity of the following: (\*) the  $\nu(\text{CO})$  mode of acetyl species at  $1595\text{ cm}^{-1}$ ; (●) the  $\nu(\text{CO})$  mode of  $\eta^2$ -acetaldehyde at  $1400\text{ cm}^{-1}$ ; ( $\triangleright$ ) the  $\nu(\text{CO})$  mode of  $\text{CO}(\text{a})$  near  $1815\text{ cm}^{-1}$ ; and (○) the intensity of the elastic peak. The data were collected in a single experiment that consisted of cycles of annealing to progressively higher temperatures and quenching the reaction by cooling rapidly to 170 K.

$\text{cm}^{-1}$  on Rh(111)<sup>36</sup> and at  $1425\text{ cm}^{-1}$  on Ru(0001).<sup>30</sup> The frequency of the CO stretch of the acetyl species in this study is consistent with coordination of acetyls on Pd(111) primarily through the carbonyl carbon, with some overlap between the carbonyl  $\pi^*$  orbital and the metal d orbitals.

Experiments were conducted to determine the temperature dependence of the intensity of the CO stretching modes of adsorbed  $\eta^2$ -acetaldehyde, acetyl, and CO species. The results of these experiments for  $\text{CH}_3\text{CHO}$  and  $\text{CD}_3\text{CDO}$  are shown in Figures 7 and 8, respectively. The data in these figures have not been normalized with respect to the corresponding elastic peak intensities in order to illustrate clearly the differences between the spectra of acetyl and acetaldehyde species. Normalization would also remove the apparent maximum in acetyl concentration with temperature. Although the vibration observed at  $1390\text{ cm}^{-1}$  in the  $\text{CH}_3\text{CHO}$  spectrum was due to both the  $\nu(\text{CO})$  and  $\delta(\text{CH}_3)$  modes of  $\eta^2$ -acetaldehyde, little reduction in the intensity of this mode was observed for  $\text{CD}_3\text{CDO}$ , suggesting that this loss was predominantly due to the  $\nu(\text{CO})$  mode of  $\eta^2$ - $\text{CH}_3\text{CHO}$ . The intensities of the CO stretch of  $\eta^2$ - $\text{CH}_3\text{CHO}$  ( $1390\text{ cm}^{-1}$ ) and  $\text{CH}_3\text{C}=\text{O}$  ( $1565\text{ cm}^{-1}$ ) species displayed significantly different temperature dependences, providing further support for the assignment of these modes to two different adsorbed species. Similar trends were observed for the CO stretch of  $\eta^2$ - $\text{CD}_3\text{CDO}$  ( $1400\text{ cm}^{-1}$ ) and  $\text{CD}_3\text{C}=\text{O}$  ( $1595\text{ cm}^{-1}$ ). The relative intensities of both the  $\nu(\text{CO})$  mode of  $\eta^2$ -acetaldehyde and the  $\nu(\text{CO})$  mode of surface acetyl species decreased above 300 K. Desorption of  $\eta^2$ -acetaldehyde as observed in TPD experiments would account for the drop in intensity of the  $\nu(\text{CO})$  mode of this species, while decomposition of acetyl species would account for the disappearance of the vibrations of this adsorbate.

Virtually no molecularly adsorbed CO was produced by acetaldehyde decomposition below 300 K. However, above 300 K the intensity of the  $\nu(\text{CO})$  mode of adsorbed CO increased rapidly

(32) Booth, G.; Chatt, J. *J. Chem. Soc. A* **1966**, 634.

(33) Adams, D. M.; Booth, G. *J. Chem. Soc.* **1962**, 1112.

(34) Werner, H.; Bertleff, W. *J. Chem. Res., Synop.* **1978**, 201.

(35) Maitlis, P. M.; Espinet, P.; Russell, M. J. H. In *Comprehensive Organometallic Chemistry*; Pergamon: New York, 1982; Vol. 6, p 279.

(36) Houtman, C. A.; Barteau, M. A., unpublished results.

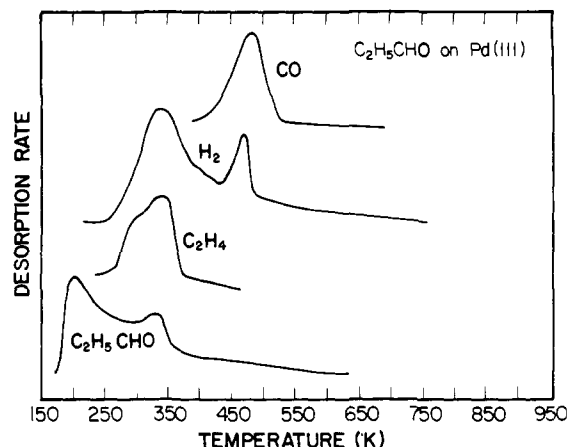
**Table IV.** Vibrational Assignments for Acetaldehyde Adsorbed on Clean Pd(111)

| mode                                | frequency, cm <sup>-1</sup> |                     |                                  |                                     |
|-------------------------------------|-----------------------------|---------------------|----------------------------------|-------------------------------------|
|                                     | Pd(111)                     |                     |                                  |                                     |
|                                     | CH <sub>3</sub> CHO         | CD <sub>3</sub> CDO | CH <sub>3</sub> CHO <sup>a</sup> | Pd-CH <sub>3</sub> C=O <sup>b</sup> |
| $\nu(\text{CH}_3)$                  | 2990                        | 2215                | 2964<br>2918<br>2747             | c                                   |
| $\nu(\text{CH})$                    | 2850                        | 2100                | 3003                             |                                     |
| $\nu(\text{CO})$ acetyl             | 1565                        | 1595                |                                  | 1667                                |
| $\nu(\text{CO})$ $\eta^2$ -aldehyde | 1390                        | 1400                | 1722                             |                                     |
| $\delta(\text{CH}_3)$               | 1390                        | 1065                | 1431                             | 1324                                |
| $\delta(\text{CH})$                 | 1390                        | 1065                | 1389                             |                                     |
| $\rho(\text{CH}_3); \nu(\text{CC})$ | 1080                        | 975                 | 1118                             | 1073                                |
| $\nu(\text{CC}); \rho(\text{CH}_3)$ | 900                         | nr <sup>d</sup>     | 882                              | 903                                 |
| $\delta(\text{CCO})$                | 600                         | 550                 | 522                              | 571                                 |
| $\nu(\text{Pd-C})$ acetyl           | 330                         | 345                 |                                  |                                     |

<sup>a</sup>IR frequencies are for crystalline acetaldehyde and are taken from ref 38. <sup>b</sup>IR frequencies were taken from ref 33 and are for *trans*-[PdBr-(COCH<sub>3</sub>)(PEt<sub>3</sub>)<sub>2</sub>]. <sup>c</sup>The  $\nu(\text{CH})$  stretches of the acetyl ligands were not resolved from those of other hydrocarbon ligands. <sup>d</sup>nr = not resolved.

due to the decomposition of adsorbed acetyl species. An inspection of Figures 7 and 8 demonstrates that a kinetic isotope effect was present for the acetyl decomposition reaction and resulted in a higher rate of CO production from CH<sub>3</sub>CHO (as measured by the increase in the intensity of the  $\nu(\text{CO})$  mode) compared to CD<sub>3</sub>CDO. These experiments were performed with computer control of the temperature, so that the temperature history of the sample was reproduced as nearly as possible for each sequence of partial-heating experiments. The reproducibility of the position of the  $\nu(\text{CO})$  intensity vs temperature curve was found to be  $\pm 1.2$  K in a series of six repeated experiments with CH<sub>3</sub>CHO. The derivative with respect to temperature of the relative intensities of the  $\nu(\text{CO})$  mode of adsorbed CO produced during CH<sub>3</sub>C=O(a) and CD<sub>3</sub>C=O(a) decomposition therefore can be used to approximate a TPD spectrum for the decomposition of acetyl species on Pd(111). By assuming a constant frequency factor of  $10^{13}$  s<sup>-1</sup>, the activation energy ( $E_a$ ) for acetyl decomposition can be calculated by using standard formulas for the analysis of TPD data.<sup>37</sup> The activation energy difference between CH<sub>3</sub>C=O and CD<sub>3</sub>C=O decomposition was calculated to be 0.8 kcal/mol, with a value of  $E_a$  for this reaction of 20 kcal/mol. The difference of nearly 1 kcal/mol for CD<sub>3</sub>C=O decomposition versus that of CH<sub>3</sub>C=O is comparable to the difference in zero-point energies for C-D bonds versus C-H bonds. The observation of a kinetic isotope effect suggests that acetyl decomposition is initiated by carbon-hydrogen bond cleavage, followed by rapid carbon-carbon bond cleavage to produce CO(a) and adsorbed C<sub>1</sub> hydrocarbon species. Although no evidence for ketene desorption was detected in the course of the acetyl decomposition reaction on the Pd(111) surface, ketene desorption was reported to accompany the decomposition of acetyl species on the Pt(111) surface.<sup>28,29</sup>

The assignments of the remainder of the vibrations observed following the adsorption of acetaldehyde on Pd(111) are summarized in Table IV. Due to similarities in the expected vibrational frequencies of acetaldehyde and acetyl species, some modes cannot be conclusively assigned to one adsorbate. The  $\delta(\text{CCO})$  mode was observed as an intense vibration at 600 cm<sup>-1</sup> in the spectrum of CH<sub>3</sub>CHO and at 550 cm<sup>-1</sup> in the spectrum of CD<sub>3</sub>CDO. The  $\rho(\text{CH}_3)$  and  $\nu(\text{CC})$  modes are strongly coupled for acetaldehyde.<sup>38</sup> Thus, the vibration observed at 1080 cm<sup>-1</sup> in the spectrum for CH<sub>3</sub>CHO at 170 K was mainly due to the  $\rho(\text{CH}_3)$  mode, while the loss at 900 cm<sup>-1</sup> was predominantly the  $\nu(\text{CC})$  mode. The CD<sub>3</sub> rocking mode of the CD<sub>3</sub>CDO adlayer appeared at 975 cm<sup>-1</sup>, and the  $\nu(\text{CC})$  mode was not resolved. The loss at 330 cm<sup>-1</sup> in the spectrum for CH<sub>3</sub>CHO was assigned to the Pd-C stretch of the adsorbed acetyl species, providing additional support for the coordination of acetyl ligands on the

(37) Redhead, P. A. *Vacuum* 1962, 12, 203.(38) Hollenstein, H.; Gunthard, H. H. *Spectrochim. Acta* 1971, 27A, 2027.**Figure 9.** TPD spectrum for a saturation exposure of propanal on the clean Pd(111) surface at 170 K.**Table V.** Product Yields for the Reaction of Propanal on the Clean Pd(111) Surface<sup>a</sup>

| product (temp, K)  | yield |
|--|-------|
| C <sub>2</sub> H <sub>5</sub> CHO (200)                      | 0.8   |
| C <sub>2</sub> H <sub>5</sub> CHO (325)                      | 0.9   |
| C <sub>2</sub> H <sub>4</sub> (335)                          | 0.2   |
| H <sub>2</sub> (340)   | 1.8   |
| H <sub>2</sub> (465)   | 1.4   |
| CO (475)   | 1.3   |
| H <sub>2</sub> (550)   | 0.5   |
| C (a)  | 0.7   |
| total C <sub>2</sub> H <sub>5</sub> CHO adsorbed and reacted | 2.5   |

<sup>a</sup>Product yields are given in units of  $10^{14}$  cm<sup>-2</sup>.

Pd(111) surface through the carbonyl carbon. The frequency of this vibration is similar to that observed for the  $\nu(\text{Pd-CO})$  mode of adsorbed CO, as demonstrated by the spectrum recorded at 350 K, where CO and C<sub>1</sub> hydrocarbons were the only adsorbed species.

**3.3. Reaction of Propanal on Pd(111).** In a fashion analogous to that of acetaldehyde, propanal decomposed on the clean Pd(111) surface via decarbonylation to produce CO, H<sub>2</sub>, and C<sub>2</sub>H<sub>4</sub>. The TPD spectrum observed following a saturation exposure to propanal on the clean Pd(111) surface at 170 K is shown in Figure 9, and the product yields are given in Table V. Propanal desorption was observed at 200 and 325 K following propanal adsorption at 170 K. The higher temperature propanal desorption peak was due to the desorption of propanal adsorbed in the  $\eta^2$  configuration. The lower temperature propanal desorption peak most likely contained a substantial contribution from species adsorbed on the sample mounting hardware, since little  $\eta^1$ -propanal was detected by HREELS, as will be shown below. No evidence was found for the oligomerization of adsorbed propanal to form the corresponding trimers or tetramers.

The reaction pathways observed in the TPD of propanal adsorbed on Pd(111) were analogous to those reported in our previous study of 1-propanol decomposition on this surface.<sup>3</sup> Desorption-limited CO produced by propanal decarbonylation desorbed at 475 K with the characteristic first order peak shape. A portion of the hydrocarbon species produced by propanal decarbonylation desorbed as ethylene at 335 K, while the remainder underwent decomposition via surface ethylidyne (CCH<sub>3</sub>) and acetylide (CCH) species. The recombination of hydrogen atoms released to the surface by propanal decomposition and ethylidyne formation occurred at 340 K. The onset of H<sub>2</sub> desorption was 250 K, slightly higher than that observed for H<sub>2</sub> produced from formaldehyde decomposition. Surface ethylidynes formed during the course of propanal conversion decomposed at 465 K, evolving H<sub>2</sub> and producing surface acetylide species. Similarly, in experiments involving ethylene adsorption on Pd(111), surface ethylidynes produced by the decomposition of di- $\sigma$ -bonded ethylene decomposed near 450 K to H<sub>2</sub> plus surface acetylide species.<sup>38,39</sup>

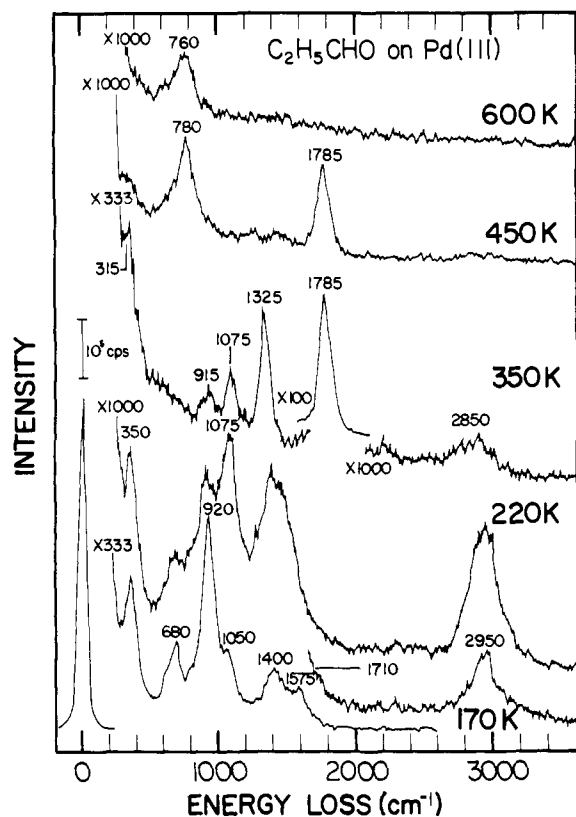


Figure 10. HREEL spectra for a saturation coverage of propanal on the Pd(111) surface at 170 K, followed by annealing to the temperature indicated.

Acetylide species produced during the course of propanal conversion on Pd(111) decomposed over a broad temperature range above 500 K and resulted in the desorption of reaction-limited  $H_2$  and the deposition of carbon atoms on the Pd(111) surface. In order to complete the desorption of  $H_2$ , the surface was heated to 1100 K in TPD experiments. Annealing the surface to this temperature caused diffusion of adsorbed carbon atoms into the bulk, resulting in a low yield for C(a), as determined by subsequent cycles of oxygen adsorption and desorption. The atomic carbon coverage reported in Table V therefore represents the lower limit of that produced from propanal.

HREELS experiments indicated that the sequence of surface reactions for propanal was analogous to that observed for acetaldehyde. The HREEL spectrum observed following propanal adsorption on the Pd(111) surface is shown in Figure 10, along with the spectra observed after annealing to higher temperatures. The adsorption of propanal on the clean surface at 170 K produced both  $\eta^2$ -propanal and propanoyl ( $CH_3CH_2C=O(a)$ ) species. The CO stretch of the  $\eta^2$ -propanal and the  $\delta(CH_3)$  and  $\delta(CH_2)$  modes of the adlayer were observed as a single peak at 1400  $cm^{-1}$ . As discussed above for acetaldehyde, the  $\nu(CO)$  mode of  $\eta^2$ -propanal can be expected to be the dominant contributor to the intensity of this loss. The CO stretching frequency of adsorbed propanoyl species was 1575  $cm^{-1}$ , consistent with the frequency of the  $\nu(CO)$  mode of surface acetyls. This frequency and the observation of the  $\nu(Pd-C)$  mode of surface propanoyls at 350  $cm^{-1}$  indicated that these species were adsorbed in essentially an  $\eta^1(C)$  configuration. Assignments of the vibrational modes observed following propanal adsorption on Pd(111) are similar to those of acetaldehyde discussed above and are summarized in Table VI.

Upon annealing the adlayer to progressively higher temperatures, vibrations of adsorbed CO were first detected at 280 K. This observation is consistent with the TPD experiments in which the onset of  $H_2$  desorption was delayed until 250 K and suggests

Table VI. Vibrational Assignments for Propanal Adsorbed on Pd(111)

| mode                      | EtCHO/Pd(111)<br>frequency, $cm^{-1}$ | EtCHO (liquid) <sup>b</sup><br>frequency, $cm^{-1}$ |
|---------------------------|---------------------------------------|---|
| $\nu(CH_3)$               | 2950                                  | 2966  |
| $\nu(CH_2)$               |                                       | 2909  |
| $\nu(CO)$ $\eta^1$ -EtCHO | 1710                                  | 1730  |
| $\nu(CO)$ acyl            | 1575                                  |   |
| $\nu(CO)$ $\eta^2$ -EtCHO | 1400                                  |   |
| $\delta(CH_3)$            | nr <sup>a</sup>                       | 1418  |
| $\delta(CH_2)$            | nr <sup>a</sup>                       | 1458  |
| $\nu_a(CCC)$              | 1050                                  | 1092, 1120  |
| $\rho(CH_3)$              | 920                                   | 898   |
| $\nu_s(CCC)$              |                                       | 660   |
| $\delta(CCO)$             | 680                                   |   |
| $\nu(Pd-C)$ acyl          | 350                                   |   |

<sup>a</sup> nr = not resolved. <sup>b</sup> IR frequencies for liquid propanal were taken from ref 40.

that the fragmentation of the adsorbed species to  $C_2$  hydrocarbons, CO, and hydrogen does not occur with an appreciable rate below 280 K. Upon annealing the adlayer to 350 K, vibrations attributed to both adsorbed  $\eta^2$ -propanal and propanoyl species disappeared completely, and the characteristic vibrations of surface ethylidyne and CO(a) were observed. The vibrational frequencies of the ethylidyne species formed by propanal decarbonylation were in excellent agreement with previous HREELS<sup>38</sup> and IR<sup>41</sup> studies of ethylidyne produced from ethylene on palladium surfaces. According to the analysis of Gates and Kesmodel,<sup>39</sup> the peak at 1325  $cm^{-1}$  was assigned to the methyl deformation mode of ethylidyne species. The ethylidyne carbon-carbon stretch was observed at 1075  $cm^{-1}$ , and the methyl rocking mode was observed at 915  $cm^{-1}$ .

Ethylidyne species produced during propanal decomposition were converted to surface acetylides (CCH) upon annealing the adlayer to 450 K. Acetylides adsorbed on the Pd(111) surface are characterized by an intense loss for the out-of-plane CCH wagging mode at 780  $cm^{-1}$  and a weak loss due to the carbon-carbon stretch of the acetylide adlayer near 1345  $cm^{-1}$ .<sup>40</sup> Angular profiles of the intensity of the observed losses demonstrated that while both modes displayed significant impact scattering character, the carbon-carbon stretch at 1345  $cm^{-1}$  displayed little dipolar character. Annealing the adlayer to temperatures above 600 K resulted in the gradual disappearance of the vibrations of the acetylide adlayer. To ensure a reproducible clean surface upon completion of HREELS or TPD experiments, the surface was annealed for 10 min at 1000 K followed by repeated  $O_2$  doses until a reproducible  $O_2$  desorption spectrum was observed with no desorption of carbon oxides detected by TPD and no surface carbon detectable by HREELS.

#### 4. Discussion

Aldehydes adsorbed on the clean Pd(111) surface displayed a rich and complex chemistry dependent upon a number of factors. The mode of coordination of the aldehyde to the surface and the structure of the group pendant from the carbonyl center had significant influences upon the reactivity of the adsorbate. Formaldehyde decomposed readily upon adsorption at 170 K via carbon-hydrogen bond cleavage to produce adsorbed CO and surface hydrogen. Polymerization of adsorbed formaldehyde to paraformaldehyde competed with the formaldehyde decomposition pathway. The paraformaldehyde adlayer decomposed near 260 K, resulting in  $H_2CO$  evolution and the release of CO and hydrogen atoms to the surface. While decomposition occurred readily for formaldehyde at 170 K, this reaction was not observed below 280 K for acetaldehyde and propanal. The decarbonylation of acetaldehyde and propanal proceeded through stable acyl species, which were identified by their vibrational spectra. Acetaldehyde

(39) Kesmodel, L. L.; Waddill, G. D.; Gates, J. A. *Surf. Sci.* **1984**, *138*, 464.

(40) Sbrana, G.; Schettino, V. *J. Mol. Spec.* **1970**, *33*, 100.

(41) Beebe, T. P., Jr.; Albert, M. R.; Yates, J. T., Jr. *J. Catal.* **1985**, *96*, 1.

(42) Sanderson, R. T. *Chemical Bonds and Bond Energy*; Academic: New York, 1971.



**Table VII.** Strengths of Selected Bonds of the Aldehydes Examined in This Work<sup>a</sup>

| compound     | bond strengths, kcal/mol |       |        |
|--------------|--------------------------|-------|--------|
|              | RC-HO                    | R-CHO | R-CCHO |
| formaldehyde | 97.2                     |       |        |
| acetaldehyde | 96.2                     | 84.6  |        |
| propanal     | 97.2                     | 84.3  | 84.3   |
| acrolein     | 98.7                     | 87.5  | 139.9  |

<sup>a</sup> Values are taken from ref 42.

reacted through acetyl species which decomposed further to release CO(a), H(a), and C<sub>1</sub> hydrocarbon species to the surface. Likewise, decomposition of propanoyl species produced during the course of propanal conversion resulted in the production of CO(a), H(a), and C<sub>2</sub> hydrocarbon species. Thus, aldehyde decomposition on the Pd(111) surface produced CO, hydrogen, and hydrocarbon species one carbon atom shorter than the parent aldehyde. Similar reaction products were observed for alcohol decomposition on Pd(111).<sup>3</sup> The results of this study provide insights into a variety of reactions involving aldehydes, including their decarbonylation, polymerization, and catalytic synthesis. These are considered in turn below.

**4.1. Aldehyde Decarbonylation.** The large differences observed in the onset of CO production from adsorbed aldehydes served to illustrate the influence of the substituent upon aldehyde reactivity. The observation of formaldehyde decomposition upon adsorption at 170 K suggests that cleavage of the acyl carbon-hydrogen bond occurred readily at this temperature. However, CO production from the higher aliphatic aldehydes adsorbed on Pd(111) was not detected by HREELS until roughly 300 K. Estimates of the bond strengths for the aldehydes examined in this study are given in Table VII. Table VII also includes the bond strengths of acrolein (CH<sub>2</sub>=CHCHO) which has been studied on the Pd(111) surface.<sup>26</sup> Acrolein decomposition produces a product slate similar to that from propanal, although the activity for ethylidene formation was higher for acrolein than for propanal. The strengths of the aldehyde carbon-hydrogen bonds for these molecules differ by only  $\pm 1$  kcal/mol, which is clearly insufficient to account for the large differences observed in aldehyde decomposition temperatures. This supports the conclusion that it is acyl decomposition rather than acyl formation which is the rate-determining step in aldehyde decarbonylation on this surface.

The stability of acyl species can be determined via HREELS by monitoring the appearance of the decomposition product CO. Figure 11 illustrates the temperature dependence of the appearance of CO following adsorption of acetaldehyde, propanal, and acrolein on the Pd(111) surface. As shown by Figure 11, adsorbed acetyl species were the most stable acyl ligands on Pd(111) and decomposed above 310 K to produce CO(a) and C<sub>1</sub> hydrocarbons. Propanoyl species were less stable and decomposed above 280 K to produce CO(a) and C<sub>2</sub> hydrocarbons. Even though the  $\alpha$  carbon-carbon bond was stronger for acrolein than for the other aldehydes, propenoyl (H<sub>2</sub>C=CHC=O) species produced from acrolein on Pd(111) were the least stable and decomposed at 260 K to produce CO(a) and CCH<sub>3</sub>(a). The low stability of propenoyls suggests that factors other than the  $\alpha$  carbon-carbon bond strength control the stability of acyl species on the Pd(111) surface.

As explained above, the derivative of the intensity of CO(a) vibrations produced by acyl decarbonylation can be used to approximate a TPD spectrum for the disappearance of acyl species. The inflection points of the intensities of CO(a) vibrations shown in Figure 11 correspond to the temperatures ( $T_p$ ) at which the rate of decomposition of each of the acyls reached a maximum. Activation energy differences for decomposition of the various acyls can be determined by using standard formulas for the analysis of TPD data,<sup>37</sup> assuming a frequency factor of  $10^{13}$  s<sup>-1</sup>. The activation energy for acetyl decomposition was calculated to be 1.6 kcal/mol greater than that for propanoyl decomposition and 3.7 kcal/mol greater than that for propenoyl decomposition.

The kinetic isotope effect observed for CO elimination from CH<sub>3</sub>CO(a) vs CD<sub>3</sub>CO(a) clearly demonstrates that C-H bond cleavage is the rate-determining step in decarbonylation of ali-

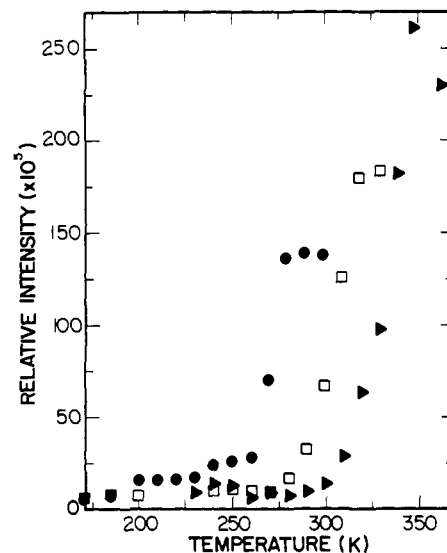


**Figure 11.** Temperature dependence of the relative intensities for CO(a) produced by the decomposition of acetaldehyde ( $\blacktriangleright$ ), propanal ( $\square$ ), and acrolein ( $\bullet$ ). The data for each aldehyde were collected in a single experiment that consisted of annealing to progressively higher temperatures, followed by cooling to 170 K.

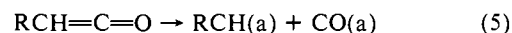
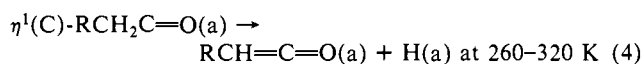
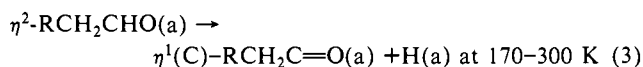
phatic acyls and that this step must precede C-C bond cleavage. This suggests that adsorbed acyls are dehydrogenated to unstable ketene species which deposit CO and the corresponding alkylidene on the surface. This sequence for acyl decomposition is consistent with the interconversion of acetyl and ketene species demonstrated on Pt(111)<sup>28,29</sup> and Ru(0001).<sup>30</sup> It may also explain the apparent inverse relationship between C-C bond strengths and activation energies for decarbonylation of acrolein vs the aliphatic aldehydes. In the case of the propenoyl species derived from acrolein, C-H bond cleavage is not necessary in order to produce unsaturated sites on the hydrocarbon backbone which can interact strongly with the metal surface. Thus C-C bond cleavage of propenoyls to yield CO plus vinyl species (which presumably isomerize rapidly to ethylidynes) can proceed directly, in effect circumventing the C-H cleavage, which is rate determining for aliphatic acyls. One would therefore expect the kinetics of propenoyl decomposition to be representative of those for C-C cleavage; the measurably lower activation energy of this reaction apparent in Figure 11 again supports the conclusion that C-H cleavage is rate-determining for decarbonylation of aliphatic acyls.

Perhaps more surprising is the high selectivity for hydrogenation of surface methylene species produced by decomposition of acetyl intermediates derived from acetaldehyde. As shown in Table III, ca. 90% of the C<sub>1</sub> species produced by acetaldehyde decarbonylation were ultimately hydrogenated to methane. We have previously demonstrated nearly stoichiometric production of methane, CO, and H<sub>2</sub> from ethanol decomposition on Pd(111). Surface methylene species are highly reactive moieties which have been successfully isolated in relatively few spectroscopic studies of surface hydrocarbon intermediates.<sup>30,43,44</sup> The hydrogenation of these species to methane is facile, as demonstrated by catalytic studies which have shown that the rate of hydrogenation of monomeric hydrocarbon species to methane on Ni surfaces is limited by the availability of adsorbed hydrogen atoms.<sup>45</sup> Likewise, if sufficient hydrogen is present on the surface from the decomposition of an organic precursor, e.g., acetaldehyde or ethanol, methane can be produced from methylene intermediates with high selectivity; if a hydrogen deficient precursor, e.g., ketene, is used, little methane is produced and dehydrogenation to atomic carbon is the fate of the methylenes.<sup>30</sup>

(43) Demuth, J. E.; Ibach, H. *Surf. Sci.* **1978**, *78*, L238.(44) McBreen, P. H.; Erley, W.; Ibach, H. *Surf. Sci.* **1984**, *148*, 292.(45) Kelley, R. D.; Goodman, D. W. In *The Chemical Physics of Solid Surfaces and Heterogeneous Catalysis*; King, D. A., Woodruff, D. P., Eds.; Elsevier: Amsterdam, 1982; Vol. 4, p 427.

Additional insights into the adsorption of aldehydes on the Pd(111) surface may be obtained through comparison with previous results for acetone on Pd(111).<sup>6</sup> Acetone adsorbed on the clean Pd(111) surface in a liquidlike phase at 170 K that contained only  $\eta^1$  species. Annealing the adlayer to 200 K converted part of the  $\eta^1$ -acetone to  $\eta^2$ -acetone, with the intensity of the  $\nu(\text{CO})$  mode of  $\eta^2$ -acetone reaching a maximum at 230 K. In contrast, HREELS experiments demonstrated that the higher aldehydes are adsorbed on Pd(111) primarily in the  $\eta^2$  configuration, even at 170 K. If the aldehydes are initially adsorbed on the Pd(111) surface in the  $\eta^1$  configuration, their conversion to the  $\eta^2$  state must be facile at 170 K. The slower conversion of  $\eta^1$ -acetone to the  $\eta^2$  configuration may be due to increased steric interactions arising from the presence of two methyl groups on the ketone compared to only one alkyl substituent on the aldehyde.

The decarbonylation of higher aliphatic aldehydes on Pd(111) thus appears to proceed via the following sequence of elementary processes:



Evidence for this sequence includes the direct observation by HREELS of  $\eta^2$ -acetaldehyde and propanal species and of the corresponding acyls and the demonstration of a kinetic isotope effect in the decarbonylation of acetyl species. As discussed above, neither the methylene nor ethylidene species postulated in step 5 were observed directly; the former were hydrogenated to methane and the latter reacted to form stable ethylidynes.

This sequence is in striking accord with the mechanistic information derived by Ponec and co-workers<sup>46,47</sup> for the synthesis of  $\text{C}_2$ -oxygenates with supported palladium catalysts. Palladium typically does not catalyze the formation of higher oxygenates from CO and  $\text{H}_2$ , owing to its lack of activity for dissociation of CO. However, these workers demonstrated that significant yields of acetaldehyde and ethanol could be produced on a Pd/ $\text{V}_2\text{O}_3$  catalyst when  $\text{CH}_2\text{Cl}_2$  was added to the feed gas. These products were *not* observed when  $\text{CH}_3\text{Cl}$  was added to the feed instead. If one assumes that methyl and methylene chlorides supply the corresponding methyl and methylene groups to the surface, respectively, these results indicate that higher oxygenates are synthesized by CO addition to alkylidene, rather than alkyl species. This proposed synthesis reaction is precisely the reverse of reaction 5 in the decomposition of acyls via ketene species above.

Evidence for the reverse of other reactions in the sequence above on palladium catalysts may also be found in the literature of catalytic hydrogenation. The reduction of acyl halides to aldehydes with supported palladium catalysts is commonly referred to as the Rosenmund reduction.<sup>48</sup> This reaction occurs under quite mild conditions (room temperature, 1 atm<sup>49</sup>) and may be used to produce aldehydes in high yield (ca. 80%<sup>50</sup>). This reaction proceeds via hydrogenation of acyl species, i.e., the reverse of step 3 above. Palladium is the most selective of the noble metals in stopping the hydrogenation at the aldehyde product rather than the alcohol, and even palladium is typically "poisoned" with sulfur and/or nitrogen compounds to improve the selectivity toward

aldehydes.<sup>48-50</sup> These catalyst characteristics may also be explained by spectroscopic studies of the interaction of carbonyl compounds with metal surfaces. Palladium exhibits less back-bonding with adsorbed aldehyde and acyl species than other group VIII metals, as evidenced by the higher frequency of the  $\nu(\text{CO})$  mode of  $\eta^2$ -aldehydes and acyls on this metal. Likewise, surface modifiers may reduce the magnitude of the enthalpy of adsorption of the product aldehydes by increasing their preference for  $\eta^1$  over  $\eta^2$  coordination, thus reducing their undesired further hydrogenation. Again the chemistry of supported palladium catalysts is entirely consistent with and is illuminated by the conclusions of these studies of the interactions of carbonyl compounds with palladium single crystals.

**4.2. Aldehyde Polymerization.** The observation of formaldehyde polymerization on the Pd(111) surface is indicative of strong interactions between formaldehyde molecules and is consistent with a body of evidence from HREELS studies on other metals. Formaldehyde polymerization has been observed previously on clean surfaces of Pt(111)<sup>21</sup> and Ni(110)<sup>22</sup> at 100 K. In both cases, formaldehyde decomposition pathways were observed in parallel with polymerization on these metals. In contrast, on the clean Ag(110) surface, formaldehyde adsorbed molecularly at 100 K and no evidence was found in HREELS and TPD experiments for either decomposition or polymerization reactions. However, the presence of adsorbed oxygen at concentrations as low as 0.05 monolayer was found to initiate formaldehyde polymerization to monolayer coverages on the Ag(110) surface.<sup>51,52</sup> Likewise adsorbed oxygen atoms increased the relative intensity of vibrations of paraformaldehyde in studies of formaldehyde adsorption on the oxygen-dosed Pd(111) surface.<sup>19</sup> These results suggest that formaldehyde polymerization requires an initiator, but that the reaction proceeds rapidly thereafter.

Formaldehyde decomposition on Pd(111) can be expected to proceed through formyl species by analogy with the reaction of the other aldehydes on this metal. A similar conclusion can be drawn for formaldehyde on the Ni(110) and Pt(111) surfaces, since the behavior of aldehydes on these metals appears to be similar to that observed on Pd(111). A possible explanation for the observation of formaldehyde polymerization on Pd(111), Pt(111), and Ni(110) surfaces is that polymerization is initiated by formyl species produced during the course of formaldehyde decomposition. In the absence of formaldehyde decomposition to formyls, as on the clean Ag(110) surface, no polymerization occurs.<sup>51</sup> By analogy with acetyl and propanoyl species, formyl groups would be expected to bind to the Pd(111) surface primarily through the carbon atom. The oxygen atom would be free to interact with neighboring formaldehyde molecules, which may lead to polymerization. This mechanism is somewhat analogous to that proposed by Stuve et al. for formaldehyde polymerization on the oxygen-dosed Ag(110) surface.<sup>51</sup> An apparent counterexample may be found in the data of Sexton et al., who reported paraformaldehyde formation on a nominally clean Cu(110) surface without any evidence for formaldehyde decomposition.<sup>53</sup> However, these experiments were apparently performed in the presence of subsurface oxygen, which oxidized a small amount of the formaldehyde adlayer to formate species, detected by their characterization decomposition to liberate  $\text{CO}_2$  at 470 K in TPD experiments. Thus, formaldehyde polymerization on the Cu(110) surface may also require initiation by oxygen.

The polymerization of higher aldehydes on metal surfaces has not been reported with the same consistency as that of formaldehyde, and polymeric species do not appear to be required to explain either the TPD or the HREEL spectra of acetaldehyde and propanal in the present study. The differences between the polymerization activities of formaldehyde and the higher aliphatic aldehydes may be attributed to unfavorable steric interactions arising from the presence of alkyl substituents. These differences

(46) Favre, T. L. F.; van der Lee, G.; Ponec, V. *J. Chem. Soc., Chem. Commun.* **1985**, 230.

(47) van der Lee, G.; Ponec, V. *Catal. Rev.-Sci. Eng.* **1987**, 29, 183.

(48) March, J. *Advanced Organic Chemistry*; McGraw-Hill: New York, 1977; p 405.

(49) Carey, F. A.; Sundberg, R. J. *Advanced Organic Chemistry; Part B*; Plenum: New York, 1977; p 78.

(50) Wheeler, O. H. In *The Chemistry of Acyl Halides*; Patai, S., Ed.; Interscience: New York, 1972; p 231.

(51) Stuve, E. M.; Madix, R. J.; Sexton, B. A. *Surf. Sci.* **1982**, 119, 279.

(52) Barteau, M. A.; Madix, R. J. In *The Chemical Physics of Solid Surfaces and Heterogeneous Catalysis*; King D. A., Woodruff, D. P., Eds.; Elsevier: Amsterdam, 1982; Vol. 4, p 95.

(53) Sexton, B. A.; Hughes, A. E.; Avery, N. R. *Surf. Sci.* **1985**, 155, 366.

are in keeping with well-established principles of polymer chemistry. While formaldehyde will readily polymerize into linear chains of the form  $(\text{H}_2\text{CO})_n$  that are stable above room temperature, analogous polymers of the higher aldehydes may be found in solution only at low temperatures in the presence of an initiator.<sup>54,55</sup> Higher aldehydes tend to oligomerize to trimers and tetramers. The two most stable oligomers of acetaldehyde are paraldehyde (2,4,6-trimethyl-1,3,5-trioxane) and metaldehyde (2,4,6,8-tetramethyl-1,3,5,7-tetroxocane). The absence of acetaldehyde oligomerization on the Pd(111) surface may be due to a barrier to trimer and tetramer formation from acetaldehyde strongly bound to the surface in the  $\eta^2$  configuration. Similar conclusions may be drawn from the results of previous TPD studies on the Ni(100) surface. Polymerization of acetaldehyde was not observed on the clean Ni(100) surface,<sup>7</sup> where the acetaldehyde desorption behavior indicates a preference for  $\eta^2$  coordination. However, on the sulfur-dosed Ni(100) surface, a significantly higher concentration of  $\eta^1$ -acetaldehyde can be inferred from TPD experiments and oligomerization to paraldehyde was observed.<sup>7</sup> This observation suggests that oligomerization is favorable only for aldehydes adsorbed in the  $\eta^1$  state.

Additional evidence supporting the conclusion that the higher aldehydes do not polymerize on the Pd(111) surface at 170 K was obtained from HREELS studies of alcohol decomposition. HREEL spectra which were virtually identical with those in Figures 5 and 10, assigned to acyl and  $\eta^2$ -aldehyde species, were obtained following adsorption of ethanol or 1-propanol on Pd(111) at 170 K and heating to ca. 200–220 K.<sup>26</sup> Previous TPD experiments have shown that the total amount of alcohol reacted via  $\eta^2$ -aldehyde intermediates was ca. 10–15% of a monolayer in each case.<sup>3</sup> In contrast, as noted above, the HREEL spectrum produced by adsorption and reaction of methanol under similar conditions corresponded to  $\eta^2$ - $\text{H}_2\text{CO}$ <sup>26</sup> and did *not* resemble that observed following  $\text{H}_2\text{CO}$  adsorption at 170 K, which we have assigned to paraformaldehyde. These results again suggest that formaldehyde alone polymerizes at 170 K on Pd(111); adsorption of higher aldehydes or production of aldehydes from aliphatic alcohols on this surface yields only  $\eta^2$ -aldehydes or their decomposition products.

White and co-workers<sup>56</sup> have recently presented evidence for formation of acetaldehyde polymers on Ru(0001) at 110 K. At

(54) Stevens, M. P. *Polymer Chemistry: An Introduction*; Addison-Wesley: Reading, MA, 1975.

(55) Allcock, H. R.; Lampe, F. W. *Contemporary Polymer Chemistry*; Prentice-Hall: Englewood Cliffs, NJ, 1981.

(56) Henderson, M. A.; Zhou, Y.; White, J. M. *J. Am. Chem. Soc.*, submitted for publication.

low coverages acetaldehyde polymerizes across the surface, while at multilayer coverages a three-dimensional polymer is formed. Their spectra for the "across-the-surface" acetaldehyde polymer are quite similar to those of Figures 5 and 6, assigned to acetyl and  $\eta^2$ -acetaldehyde species, and include interse losses at 605 and 1095  $\text{cm}^{-1}$ , which they assign to the  $\delta(\text{OCO})$  and  $\nu_s(\text{OCO})$  modes of the polymer species<sup>56</sup> (cf. Table II). However, on Ru(0001) these losses disappear upon heating to 250 K,<sup>56</sup> whereas they persist on Pd(111) at temperatures above 300 K. Since this temperature exceeds both that at which acetaldehyde polymers decompose in solution and that at which paraformaldehyde (which would be expected to be more stable than acetaldehyde polymers) decomposes on Pd(111), it does not appear plausible to assign features in the HREEL spectra of Figures 5 and 6 to acetaldehyde polymers. It is conceivable that such species might form on Pd(111) at lower temperatures and/or multilayer coverages; however, these conditions were not accessible in the present study.

## 5. Summary

The presence of alkyl substituents had a dramatic effect upon the reaction of aldehydes on the clean Pd(111) surface. Adsorbed formaldehyde either decomposed to CO(a) and H(a) or underwent polymerization to paraformaldehyde upon adsorption at 170 K. The reaction of formaldehyde on the Pd(111) surface most likely involved formyl species which either decomposed to CO and  $\text{H}_2$  or initiated formaldehyde polymerization. Significantly different behavior was observed for the higher aldehydes. Decarbonylation of adsorbed  $\eta^2$ -acetaldehyde and  $\eta^2$ -propanal proceeded through stable acyl species and resulted in the production of CO,  $\text{H}_2$ , and a hydrocarbon one carbon atom shorter than the parent aldehyde. The stability of acyl intermediates in the aldehyde decarbonylation reaction was found to depend upon the identity of the substituent group and decreased in the order: acetyl ( $\text{CH}_3\text{C}=\text{O}$ ) > propanoyl ( $\text{CH}_3\text{CH}_2\text{C}=\text{O}$ ) > propenoyl ( $\text{CH}_2=\text{CHC}=\text{O}$ ) > formyl ( $\text{H}-\text{C}=\text{O}$ ). A kinetic isotope effect was observed in the decomposition of acetyl species derived from  $\text{CH}_3\text{CHO}$  and  $\text{CD}_3\text{CDO}$ , suggesting that this reaction proceeds via unstable ketene intermediates.

**Acknowledgment.** We wish to thank Prof. R. F. Heck for helpful discussions concerning the chemistry of palladium coordination compounds. We would also like to thank Prof. J. M. White for sharing a preprint of ref 56 with us prior to its submission. This work was supported by the Division of Chemical Sciences, Office of Energy Research, U.S. Department of Energy (Grant FG02-84ER13290).

**Registry No.**  $\text{H}_2\text{CO}$ , 50-00-0;  $\text{CH}_3\text{CHO}$ , 75-07-0;  $\text{C}_2\text{H}_5\text{CHO}$ , 123-38-6;  $\text{D}_2$ , 7782-39-0.

## Radical-Cation Acidities in Solution and in the Gas Phase

F. G. Bordwell\* and Jin-Pei Cheng

Contribution from the Department of Chemistry, Northwestern University, Evanston, Illinois 60208. Received June 29, 1988

**Abstract:** The acidities of radical cations derived from PhSH, PhOH, cyclopentadiene, PhCH<sub>2</sub>CN, fluorene, PhNH<sub>2</sub>, Ph<sub>2</sub>CH<sub>2</sub>, and PhCH<sub>3</sub> have been estimated in Me<sub>2</sub>SO and in the gas phase by combination of acidity data for the parent acids ( $\text{p}K_{\text{HA}}$ ) with oxidation potentials for HA [ $E_{\text{ox}}(\text{HA})$  in Me<sub>2</sub>SO and IP(HA) in the gas phase] and with oxidation potentials for A<sup>-</sup> [ $E_{\text{ox}}(\text{A}^-)$  in Me<sub>2</sub>SO and EA(A<sup>-</sup>) in the gas phase]. The acidity order in the two media was found to be nearly the same and a near-linear correlation between the two sets of data was obtained. Structural effects on the acidities of the parent acids, HA, and on the acidities of the radical cations, HA<sup>•+</sup>, in the two media are discussed.

Although proton transfer from radical-cation intermediates is often an important step in the oxidation of organic molecules, explorations of acid-base equilibria involving these transient species (eq 1) remain as a relatively untouched area.<sup>1</sup> Measurement of



the position of such equilibria presents a challenging problem because the radical species present on either side in eq 1 are highly reactive and short-lived, which makes establishment of the

(1) Hammerich, O.; Parker, V. D. *Adv. Phys. Org. Chem.* 1984, 20, 50-187.